ISSN 0252-1075
Research Report No. RR-076

Contributions from
Indian Institute of Tropical Meteorology

SIMULATION OF MONSOON TRANSIENT DISTURBANCES IN A GCM

by

K. ASHOK,
M.K.SOMAN,
and
V. SATYAN

PUNE - 411 008
INDIA

AUGUST 1998

CONTENTS

** Figures comprise of 21 pages and can be accessed from page 18. All figures have Descriptive Legends.*

Simulation of Monsoon Transient Disturbances in a GCM

K. Ashok, M. K. Soman & V. Satyan

Indian Institute Of Tropical Meteorology , Pune - 411 008

ABSTRACT

A large part of the rainfall over India during the summer monsoon season (June-September) is distributed by synoptic scale disturbances such as monsoon depressions. To study the evolution of such disturbances in Atmospheric General Circulation Models (AGCM), the Hadley Centre AGCM (HadAM2b) has been integrated for 15 summer monsoons (1979-1993) and the output was examined for the presence of synoptic scale disturbances like monsoon depressions, Low Pressure Areas, Land Lows and Land Depressions over the Indian summer monsoon region. The atmospheric initial condition for each of these integrations was 23 May and observed SSTs were prescribed as boundary condition.

Although the horizontal resolution of the AGCM used in this study is only 2.5°x3.75° lat long., the model is able to simulate a few monsoon disturbances. The important features of these simulated disturbances are presented. The features of the simulated disturbances are realistic. The morphologies of a well simulated monsoon depression and a simulated low pressure area are presented as examples. The frequency of the simulated monsoon depressions is less than the climatological frequency of the depressions during all the four monsoon months.

1. INTRODUCTION

Monsoon Depressions and other transient disturbances that form over the Bay of Bengal and move westwards are an important component of the Indian Summer Monsoon. They play a vital role in the distribution of the rainfall during this season over the Indian region. The monsoon depressions originate near the Head Bay of Bengal during July and August and over the Central Bay during the months of June & September. They move west-northward along the monsoon trough towards the heat low system over the north-west India and Pakistan. The climatological life expectancy of a monsoon depression varies from 2 to 5 days. The frequency is about 2 depressions during every monsoon month (Sikka, 1977). Their formation is favoured by conditions like high Sea Surface Temperatures (~29 C), the dipping of the monsoon trough into north Bay of Bengal, a favourable alignment of upper anticyclonic circulation etc. (Sikka, 1977). Very few monsoon depressions reach the strength of the tropical cyclones.

Only a few studies have been reported on the simulation of transient disturbances in AGCMs. Haarsma et al. (1993) studied the evolution of tropical cyclones, their tracks and the possible effect of the doubling of carbon-dioxide on their evolution and frequency. Lal et al. (1995) used a high resolution AGCM to study the synoptic scale monsoon disturbances. Their study examined the impact of doubling of carbon-dioxide on the evolution of these disturbances. Ashok et al. (1998) obtained some preliminary results of monsoon depression simulation by a GCM. The results showed that the model they used is able to simulate some features of monsoon depressions.

The aim of the present study is to investigate the evolution of monsoon transient disturbances as simulated by the Hadley Centre AGCM by analysing model output from a large number of simulations. Simulations for 15 summer monsoon seasons from 1979 to 1993 were examined in this study. Seasonal forecasting of monsoon rainfall over India using GCMs is a topic of great current research interest. It was felt that if the model is able to simulate the monsoon depressions and their evolution satisfactorily, it would validate the physics of the model giving greater credibility to the seasonal forecasting.

2. THE MODEL

The model used in this study is the Hadley Centre AGCM version HadAM2b. The resolution of this model is 2.5° in latitude (73 rows) x3.75° in longitude (96 columns). This is a primitive equations model written in spherical polar co-ordinates with a complete representation of the Coriolis force. A hybrid vertical co-ordinate system is used. It's values at every level is a function of the sigma and pressure values. It is equal to unity at the lower boundary and equal to a multiple of the surface pressure at the upper levels. The present version has 19 vertical levels. Bottom four levels are pure sigma levels and with a smooth transition top four levels are chosen to be pressure levels. A regular latitude-longitude grid is used in the horizontal with variables arranged according

to the Arakawa B grid. The thermodynamic variables are placed at the centre of the grid cell with wind components at the corners.

A split-explicit finite difference scheme is used to integrate the equations in time (see Cullen & Davies, 1991). The solution part is split into two parts; the geostrophic adjustment process is separated from the advection part. Averaged velocities over the three adjustment time-steps are used for advection which is integrated in time using the Heun scheme. The finite difference scheme is fourth order accurate in space. The vertical velocity vanishes at both top and lower boundaries. The important predicted fields are surface pressure, horizontal components of the wind and two conservative thermodynamic variables 'liquid water potential temperature' and 'total water mixing ratio' related to the potential temperature and specific humidity via the cloud content. Apart from these variables some other primary variables like soil moisture, snow depth, surface temperature etc. can be calculated. A 30 minute time-step is used to compute field increments from both dynamical and physical routines although full radiation calculations are performed only at every three hours for economy.

Some of the physical parameterization schemes of the model are briefly discussed below:

(i) **Boundary Layer & Land-Surface processes**

The boundary layer is designed to occupy upto 5 layers of the model atmosphere. A first order turbulent mixing scheme is used to mix the conserved thermodynamic variables and momentum in the vertical (Smith, 1990). The presence or absence of cloud is accounted while calculating the transport coefficients. Over the land, surface roughness characteristics are prescribed according to climatological surface type. On the oceans, these are calculated from local wind speeds using the Charnock formula (Charnock, 1955). The boundary layer is formulated in terms of conserved variables and so can represent both dry and cloudy boundary layers (Smith, 1994). A multi-layer soil temperature scheme and a complete hydrology scheme are included (Warrilow et al., 1986). A model of the vegetation canopy is also included in the model. Moisture can be retained in the canopy or transferred to the soil or the atmosphere. Different vegetation types are included. A distribution of rainfall rate within each grid box rather than a uniform value is assumed (Dolman and Gregory, 1992).

(ii) ***Large-scale Cloud & Precipitation***

Large-scale clouds (Smith, 1990, Smith and Gregory, 1990) are represented by their liquid water (or ice) content. Large-scale precipitation is calculated in terms of water or ice-content of the clouds; frozen cloud fall out scheme allows cloud ice to contribute to the water and ice budget of lower levels as it falls. Cooling of the atmosphere due to evaporation of precipitation is included.

(iii) ***Convection***

Model uses a mass flux convection scheme (Gregory and Rowntree, 1990). The mass flux convection scheme represents both dry and moist convective processes and is designed to simulate the effects of shallow, mid-level and deep convection upon the large-scale flow. Here the magnitude of convective activity is calculated by considering the stability of lowest convective layers only.

The scheme represents an ensemble of clouds using a bulk one-dimensional cloud, based upon parcel theory, modified by entrainment and detrainment. Thus the

parcel characteristics calculated by the cloud model represent average over the entire ensemble. Provision for convective downdrafts also exists.

(iv) Radiation

The scheme consists of two parts, solar radiation and the long-wave radiation. The scheme uses four spectral bands for solar radiation as defined by Slingo (1989) and six bands for long-wave radiation (Slingo and Wilderspin, 1986). Both diurnal and annual cycles of insolation are represented with the incoming solar radiation rescaled on each physics time step to give more smoothly varying radiative forcing during day light. It allows water vapor, ozone, carbon dioxide and large-scale convective cloud distribution. Cloud radiative properties depend on cloud water and ice content and the optical thickness of clouds.

(v) Gravity Wave Drag

The effect of gravity wave is applied to the momentum components in the free atmosphere using a parameterization based on a prescribed sub-grid scale orographic variance field and the vertical stability profile as a function of height throughout the atmospheric column (Palmer et al., 1986).

(vi) Eddy diffusion

Horizontal eddy diffusion is represented by simple subgrid filters. The filters can be iterated to make them more scale selective for use at low resolution (Cullen and Davies, 1991). Vertical eddy diffusion is sometimes necessary to remove oscillations caused by inadequately resolved quasi-inertial waves. Only winds are smoothed (Wilson 1990).

Further details can be obtained from Johns (1996).

3. METHODOLOGY

The criteria we have adopted for identification of the monsoon depressions in the model output is similar to the definition used by India Meteorological department (IMD) i.e. the wind speed should be between 17-33 knots and a horizontal pressure-gradient of 5-13 hPa from the centre to about 250 km. Different features of the monsoon depressions like the vertical extent of cyclonic vorticity, rainfall distribution, vertical distribution of the temperature anomalies in the core region were examined and compared with the observational features (Godbole, 1977 and Sikka, 1977).

In Ashok et al. (1998) the model was integrated with the initial atmospheric conditions of 1 June 1991 and the simulation was continued upto 1 Oct., 1994. The model output was analyzed for the presence of the monsoon transient disturbances, their evolution and morphological features. The results showed that the model is able to simulate the monsoon depressions reasonably well. Features like distribution of vorticity at different levels, precipitation distribution within the disturbance and temperature anomaly distribution in vertical were comparable in general with those of the observed monsoon disturbances.

In the present study the integrations of 15 monsoon seasons from 1979 to 1993 were analyzed with the same objective of studying monsoon depressions and lows. The initial condition of each of these integrations is May 23 of the respective year. Observed global SST fields for these years were used as boundary conditions. Other boundary conditions like snow cover etc. are climatological.

4. RESULTS

Daily surface pressure, 850 hPa wind fields and rainfall for each of the 15 simulated monsoon seasons have been examined to identify lows and depressions that formed over the Indian region.

4.1 Frequency of the disturbances

About 2-2.5 depressions form during each month of the monsoon season. It is probable at 80% that at least a single disturbance would form during a monsoon month. The probability of formation of four or more of monsoon depressions in a monsoon month is very less (Sikka, 1977).

Table 1 gives the yearly frequency of different categories of the model generated cyclonic disturbances. In the table these disturbances are classified based on the closed isobars of surface pressure drawn at 2 hPa intervals. In Table 1, SCIL stands for Single Closed Isobaric Low. DCIL stands for Double Closed Isobaric Low. Depression is the Monsoon Depression. Land Lows and Land Depressions are closed low pressure areas and Depressions which formed over the land. From the table it is clear that the model is able to simulate mainly low intensity disturbances. The frequency of monsoon depressions is much lower than the climatological number of depressions (2 to 2.5) per season. Apart from the disturbances included there were some other disturbances that crossed well south of 15 N which are not presented in this table. These type of disturbances were maximum during the month of September and were of the post-monsoonal type.

Table 2 gives the monthwise break-up of the different types of disturbances summed over the fifteen years. The model tends to simulate almost the same number of disturbances in all the months except in June. However, the number of low pressure areas forming over the land is higher in the second half of the monsoon season.

4.2 Daily Morphological features of the simulated Monsoon Disturbances

In monsoon depressions circulation is cyclonic upto 1000 km in the horizontal and upto 9 km in the vertical. Maximum cyclonic components are observed in general between 0.9 km-1.5 km in the vertical and about 300-400 km from the centre. Maximum cyclonic wind strength reaches upto 15 m/s. The anticyclonic flow aloft is seen at about 10 km. The maximum anticyclonic winds of about 8 m/s are seen at the height of 12 km, 500-600 km away from the centre. The depressions show little tilt upto 500 hPa but markedly to the south-east between 500-300 hPa. A strong vortcity core of 12-15 $x10^{-5}$ /s is observed at the centre of the depression near the surface (Sikka, 1977).

Rainfall maxima in monsoon depression mainly occurs in southern and eastern sectors of the depression when the depression is over the Bay of Bengal and in the southwest quadrant when the disturbance moves or lays farther west over the central or western part of the Indian region. The zone of maximum rainfall shifts to northwest and then to northeast when the disturbance changes its direction from northwest to north and then to northeast. 24-hour accumulated rainfall in a depression typically ranges between 10-20 cm. Isolated rainfall amounts of 30-40 cm have been also recorded. Monsoon depressions have a cold core in the lower troposphere upto 600 hPa and warm core aloft.

Over the Arabian sea, warmer temperatures are only found to the west of the depression centre. In the observed case of a depression (Sikka, 1977) the thermal amplitude in the lower levels was found to be as high as 6 C, if the Arabian region was included in the depression environment. Excluding this region reduced the amplitude to 1-2 C in the lower levels. Warming of the same order was found in the upper troposphere.

The morphological features of simulated disturbances are comparable to those in observations. As examples, the morphologies of a well simulated monsoon depression and a Low Pressure Area during 1991 are presented below.

4.2.1 Monsoon Depression (7 -14 , July 1991):

This disturbance formed as a low pressure area centred at 91°E, 14 N on 7 July, 1991. The surface pressure distribution during this period is presented in Fig. 1. Next day it intensified at the same location into a deep depression with four closed isobars. By 10 July it further deepened, moved further north-west. Continuing to move northwest the disturbance started filling up on 11 July. By 14 July it dissipated over the Gujarat coast. The formation of another depression on 15 July also can be noted in this figure.

The corresponding daily precipitation distribution is shown in Fig. 2. By 7 July the precipitation rate has increased over the general area of the disturbance. From 8 to 11 July, the maximum precipitation rate of the above 75 mm/day is seen to the south of the track of the disturbances. The centre of the precipitation moved along with the disturbance towards northwest. Associated with the formation of the disturbance in Bay of Bengal, there is a general increase in rainfall along the west coast of peninsula. By the 12 July the total precipitation rate has decreased over the east coast in lieu with the weakening of the disturbance and the precipitation over the west coast has been increasing due to the influence of this disturbance.

The daily distribution of the windflow at 850 hPa is presented in Fig. 3. The cyclonic circulation in the region of the disturbance can be clearly seen. The westerly wind flow across the peninsula has strengthened with the intensification of the depression leading to the enhanced rainfall over the west coast.

The relative vorticity distribution at 850 hPa is shown in Fig. 4. The concentration of the cyclonic vorticity with a peak $8 x10^{-5}$ /s can be seen on 7 July at 91E, 14N. The north-west movement of the disturbance is also reflected in the movement of the vorticity centre. By 8 July a peak relative vorticity of $10 x10^{-5}$ /s was simulated by the model and this was maintained till 11 July. The simulated peak relative vorticity of $12 x10^{-5}$ /s was on 9 and 10 July. The positive relative vorticity is observed extending upto 300 hPa. The daily relative vorticity at 500 & 300 hPa levels is presented in figs. 5 & 6 respectively. Anticyclonic vorticity is observed above 300 hPa.

The vertical distribution of the latitudinal anomalies in temperature between 7-12 July, 1991 is presented in Fig. 7. Daily latitudinal means at each level are computed for the latitude passing through the centre of the disturbance. These means are calculated over the longitudinal distance of 20°, with the centre of the disturbance being at the middle of the averaging distance. The anomalies are calculated from the means at every longitude within the range of aforesaid 20° at every level.

On 7 July, the first day of the formation of the disturbance, though a clear core is not seen at the centre (91°E), lower level temperature anomalies are negative. At the centre, the cold anomalies extends upto 850 hPa and is seen to be topped by a core of warm anomalies. At the centre, the surface temperature anomaly is about -1.1 C. The maximum warm core temperature on this day is just above 1 C. By the 8 July the warm core temperature maximum has increased to 1.5 C at the height of 700 hPa at the centre (90°E). The temperature transition level between the lower cold anomalies at the centre and the upper warm core is seen at 850 hPa, as it was on the previous day. By the 9 of July the temperature transition level at the centre has reached the lowest level of about 920 hPa, signifying a strong intensification of the depression. By the 10 of July the cold anomaly at the centre of the disturbance (located at 86°E on this day) is seen upto 970 hPa. As the depression weakens the height of the temperature transition level increases to 800 hPa on 11 July at the centre of the disturbance (84°E) and upto 525 hPa on 12 July. A peak heating of 2.25 C is seen on 10 July.

Averaged morphological features:

To get an average picture of the depression, mean fields for 8 to 11 July have been computed. These are presented and discussed in this section. The averaged PMSL is presented in Fig. 8. The mean position of the disturbance during this period is seen centered at 87 E and 18 N. Because of averaging the moving depression, original intensity is not seen.

The corresponding time-averaged vertical distribution of latitudinal temperature anomalies is presented in Fig. 9. The method of averaging was analogous to the compositing technique used by Godbole (1977) to study the latitudinal anomalies of temperature in vertical. The picture presented is the time-average state of the disturbance between 8-11 July. The cold region at the centre (87 E) is seen to extend upto 900 hPa and a warm core aloft to the right, indicating the possibility of the disturbance having an eastward tilt. Observational studies have indicated that monsoon depressions tilt south east between 500-300 hPa (Sikka, 1977). The peak warm core anomaly temperature is seen to be above 1.25 C. At the surface the cold temperature anomaly is above -0.25 C

The averaged stream lines at the levels of 850, 500 & 300 hPa are presented in Fig. 10. From the picture is can be seen that the depression is tilting to south in the vertical, as in observations. Anticyclonic vorticity is present only above 300 hPa (not shown).

4.2.2 Low Pressure Area (4-9 Sep., 1991):

This low pressure area has formed over the east coast at 84.5°E and 17°N on 4 Sep., 1991 as a SCIL of 996 hPa (Fig. 11). By 6 Sep it has intensified into a DCIL with central surface pressure reaching a value less than 994 hPa. It has moved slightly north-west from its genesis location by then. By 7 Sep. the depression has moved further west and an elongated closed isobar can be seen enveloping this DCIL. The disturbance has become diffused by 8 September and has turned into a DCIL over the land, enveloping the peninsular India. It got further filled by 9 Sep. and disappeared by 10 September.

The distribution of precipitation is shown in Fig. 12. A sharp increase in precipitation occurred over the east coast of India by 4 Sep. due to the formation of the depression. It further intensified by 5th September. to a maximum of about 75 mm/day. As the

disturbance moved over the land the regions of Gujarat and surrounding regions experienced more precipitation than the previous day.

The windflow at 850 hPa is given in Fig. 13. The formation of the cyclonic circulation associated with the low pressure area on 4 September and its movement can be clearly seen from this Figure. The daily relative vorticity distribution at 850 hPa shows (Fig. 14) a strong core of cyclonic relative vorticity of about $5 x 10^{-5}$/s in the Bay of Bengal on 4 September, to slightly south-east of the surface low pressure centre. By 5 Sep. the pattern moved west and intensified to values more than $8 x 10^{-5}$/s. By 6 Sep it reached a broad peak above $8 x 10^{-5}$/s as the disturbance moved west. The relative vorticity decreased and became diffused by 8 Sep, as the depression diffused.

The daily relative vorticity distribution at 300 hPa shows that (Fig. 15) on 4 September the southern peninsula and the adjoining Bay of Bengal have cyclonic vorticity above $2 x 10^{-5}$/s. at this level. By 5 September strong cell of concentrated relative vorticity with peak above $5 x 10^{-5}$/s can be seen even the this level centred at the 81°E and 18°N . By the 6 Sep., the relative vorticity core has become more diffused as the disturbance moved west. By 7 Sep. the relative vorticity centre can be seen at 82°E and 20°N. After this day cyclonic vorticity pattern at this level has become diffused.

The low pressure area was relatively cold in lower levels and warm aloft.

SUMMARY AND CONCLUSIONS

The monsoon simulations for the years 1979 to 1993, with the initial conditions of May 23rd of every year, by the Hadley Centre AGCM was analyzed for the presence of monsoon transient disturbances. The integrations used observed global SSTs of the respective months and climatological values of other boundary conditions like soil moisture, snow cover etc.

Though the integrations were carried out at relatively coarse resolution of 2.5°X 3.75° lat-long, the model is able to simulate different transient disturbances over the Indian region reasonably well. The analyzed morphological features like surface pressure, lower tropospheric winds, relative vorticity at different levels, rainfall etc. are realistic. Two examples of the simulated disturbances have been presented in this study. However, the simulated frequency of the monsoon depressions is less than the observed frequency. The number of low pressure areas simulated by the model is much larger than the number of stronger disturbances. This may be due to the inadequate resolution of the model used in this study.

The results presented above indicate that though the AGCM at the present resolution is able to simulate some transient disturbances of monsoon seasons, to study in detail, the effect of climate change due to natural or anthropogeneic reasons on the frequency and structure of these disturbances, a much higher resolution AGCM or a limited area model nested to the AGCM with present resolution will be required.

ACKNOWLEDGMENTS

The authors are thankful to Dr. G. B. Pant, Director, Indian Institute of Tropical Meteorology, Pune, for the facilities extended to carry out the work. The authors thank the Hadley Centre for Climate Research, UK for having provided their AGCM. The work reported in this paper is carried out as part of Climate Research Project funded by the Department of Science & Technology (DST), Govt. of India. The authors thank the reviewer for his valuable comments and suggestions.

Table 1: Frequency of Systems in Different Categories

Year	SCIL	DCIL	Depressions	Land lows	Land Deps.	total
1979	4	0	0	1	0	5
1980	2	1	1	0	1	5
1981	1	0	0	1	0	2
1982	1	0	0	2	0	3
1983	7	0	0	5	0	12
1984	10	1	0	3	0	14
1985	6	1	0	4	0	11
1986	8	0	0	0	0	8
1987	7	0	0	0	0	7
1988	7	0	0	4	0	11
1989	5	0	0	2	0	7
1990	6	1	1	7	0	15
1991	5	2	4	2	0	13
1992	8	0	1	3	0	12
1993	5	1	0	1	0	7

* Grand Total - 132

Table 2: Monthwise distribution of simulated synoptic scale disturbances

Month	SCIL	DCIL	Depressions	Land lows	Land Deps.
June	13	5	1	5	Nil
July	25	0	2	7	Nil
Aug	23	0	2	11	1
Sep	21	2	2	12	Nil

REFERENCES

Ashok, K., Satyan, V., & Soman, M. K., 1998: Simulation of monsoon transient disturbances in UKMO General Circulation Model.. Accepted for publication in *Journal of Appl. Hydrology.*

Charnock, W. 1955: Wind stress over the water surface. *Quart. Jou. Roy. Met. Soc.,* **81**, 639.

Cullen, M. J. P., and Davies, T., 1991: A conservative split-explicit integration scheme with fourth order horizontal advection. *Quart. J. Roy. Met. Soc.,* **117**, 993-1002.

Dolman, A. J., and Gregory, D., 1992: The parameterization of rainfall interception in GCMs, *Quart. Jou. Roy. Met. Soc.,* **118**, 455-467.

Godbole, R. V., 1977: The composite structure of the monsoon depression. *Tellus,* 29, 25-40.

Gregory, D., and Rowntree, P. R., 1990: A mass flux scheme with representation of cloud ensemble characteristics and stability dependent closure. *Mon. Wea. Rev.,* 118, 1483-1506.

Haarsma, R. J., Mitchell, J. F. B., and Senior, C. A., 1993: Tropical disturbances in a GCM. *Climate Dynamics,* 8, 247-257.

Johns, T. C., 1996: A description of the second Hadley Centre coupled model (HADCM2). *Clim. Res. Tech. Note CRTN 71.*

Lal, M., Bengtsson, L., Cubasch., U., Esch., M., and Schlese, U., 1995: Synoptic scale disturbances of the Indian summer monsoon as simulated in a high resolution climate model. *Climate Research,* **5**, 243-258.

Palmer, T.N., Shutts, G. J. and Swinbanks, R., 1986: Alleviation of a systematic westerly bias in general circulation and numerical weather prediction models through an orographic gravity wave parameterization, *Quart. Jou. Roy. Met. Soc.,* 112, 1001-1039.

Sikka, D. R., 1977: Some aspects of the life history, structure and movement of monsoon depressions. *Pageoph,* **155**, 1501-1529.

Slingo, A., 1989: A GCM parameterization for the short wave radiative properties of water clouds. *J. Atm. Sci.*, **46**, *1419-1427.*

Slingo, A. and Wilderspin, R. C., 1986: Development of a revised long wave radiation scheme for an atmospheric GCM. *Quart. Jou. Roy. Met. Soc.*, **112**, 371-386.

Smith, R. N. B., 1990: Subsurface, surface, and boundary layer processes. *Unified Model Doc. Paper 24. Available at Nat. Met. Lib., Bracknell.*

Smith, R. N. B., and Gregory, D., 1990: Large scale precipitation. *Unified Model Doc. Paper 26. Available at Nat. Met. Lib., Bracknell.*

Smith, R. N. B., 1994: Experience and developments with layer cloud and boundary layer mixing schemes in the UKMO Unified Model: *Workshop on parameterization of the cloud topped boundary layer,* 8-11 June 1994, ECMWF.

Warrilow, D. A., Sangster, A. B., and Slingo, A., 1986: Modelling of land surface processes and their influence on European climate. *Dynamical climatology Tech. Note. No. 38, Available at Hadley Centre, UKMO.*

Wilson, C. A., 1990: Vertical diffusion. *Unified Model Doc Paper 21.*

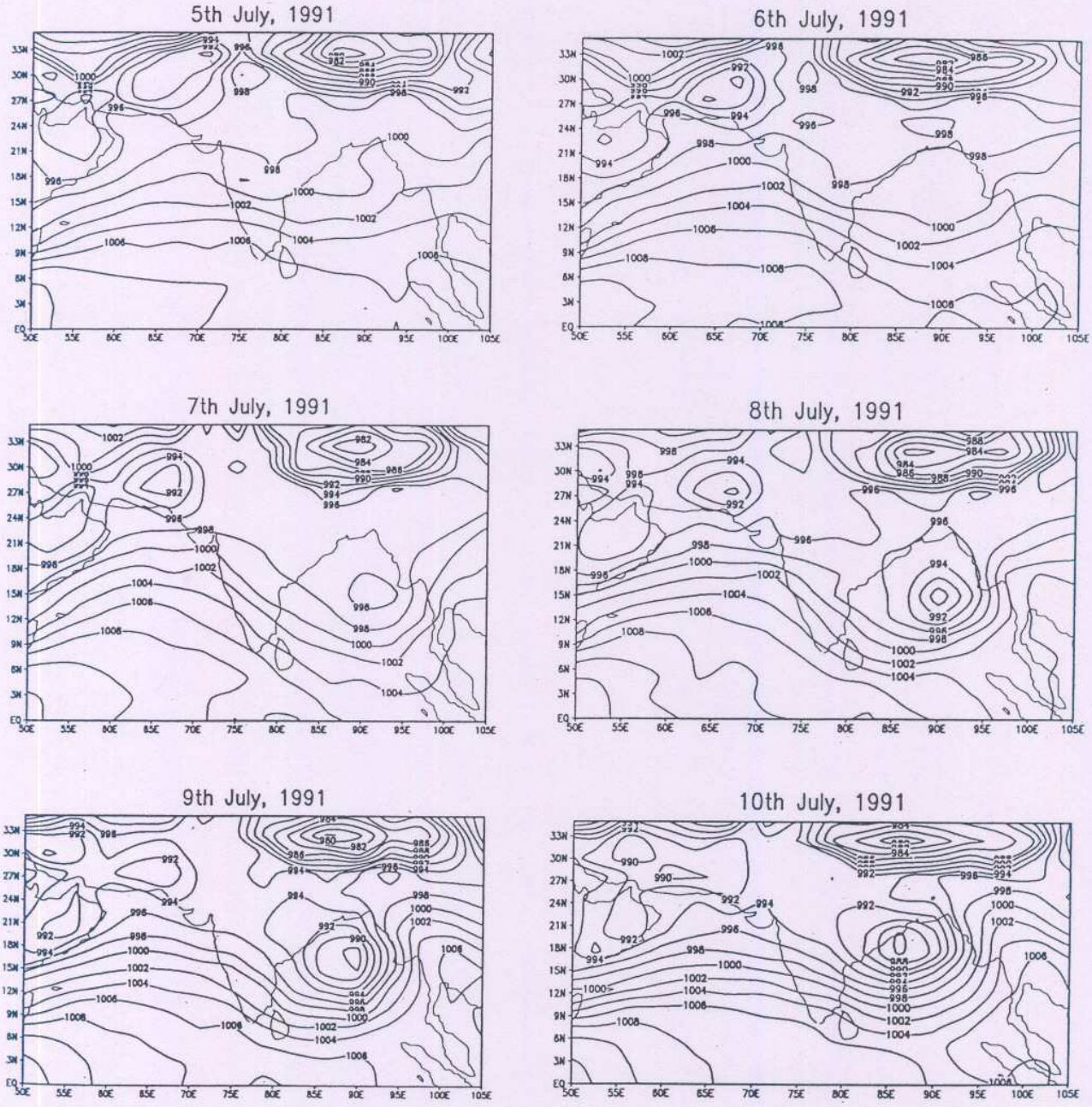

Fig. 1a :Simulated Monsoon Depression by the Hadley Centre Climate Model. Sea Level Pressure (hPa). Contour intervals at 2 hPa

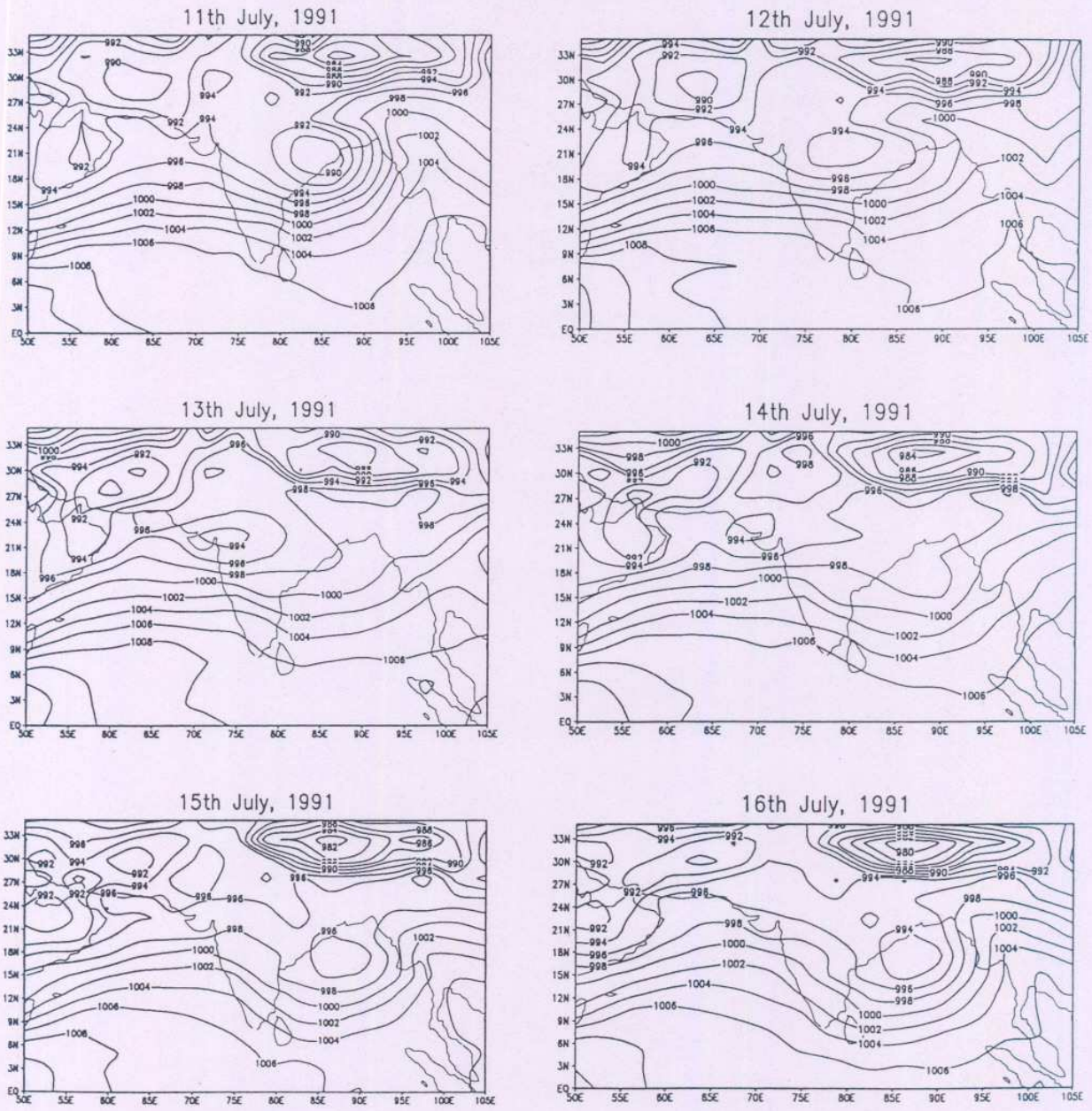

Fig. 1b Simulated Monsoon Depression by the Hadley Centre Climate Model. Sea Level Pressure (hPa). Contour intervals at 2 hPa

Fig. 2a :Simulated Monsoon Depression by the Hadley Centre Climate Model.
Daily Rainfall (mm/day)

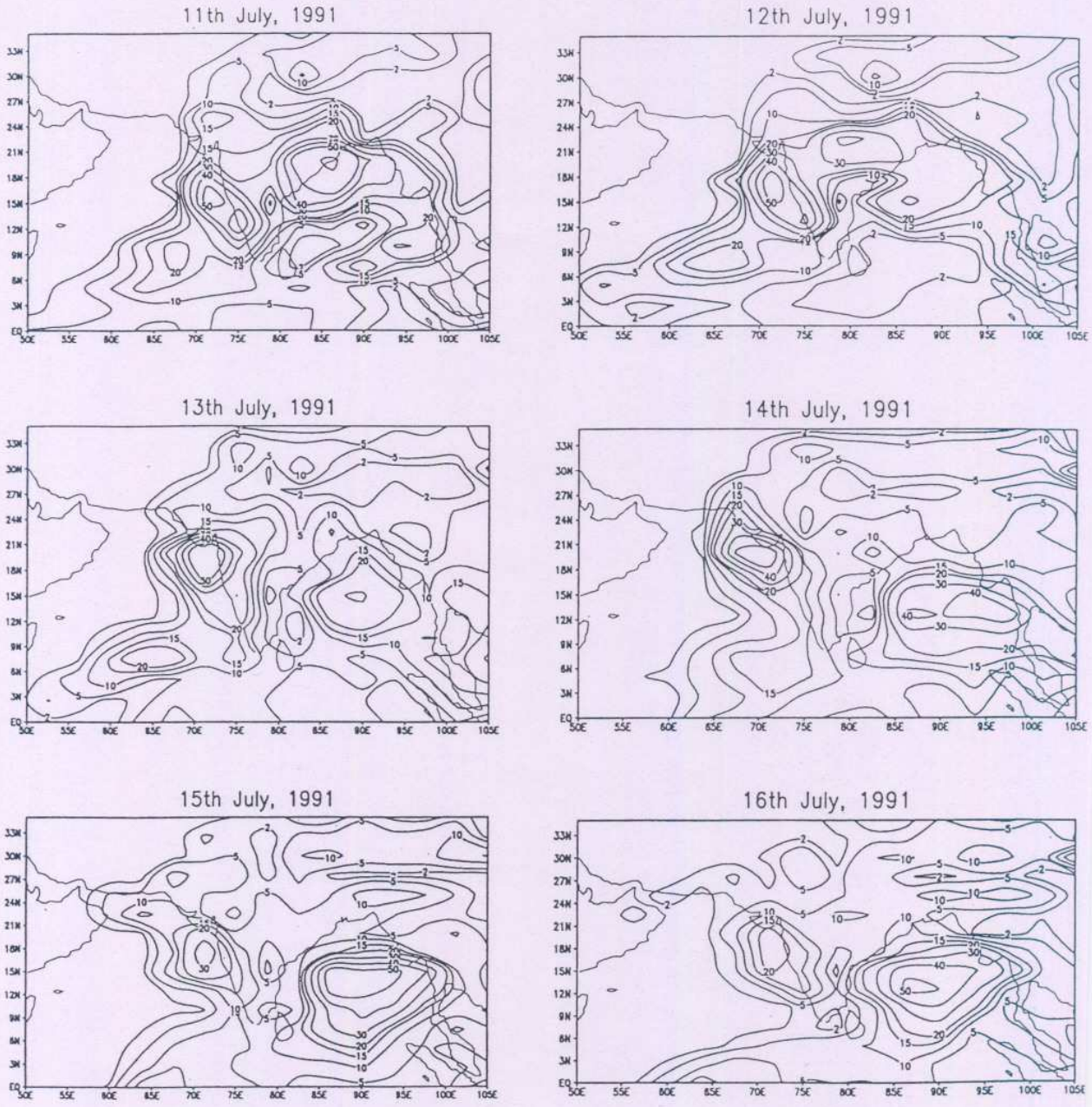

Fig. 2b Simulated Monsoon Depression by the Hadley Centre Climate Model.
Daily Rainfall (mm/day)

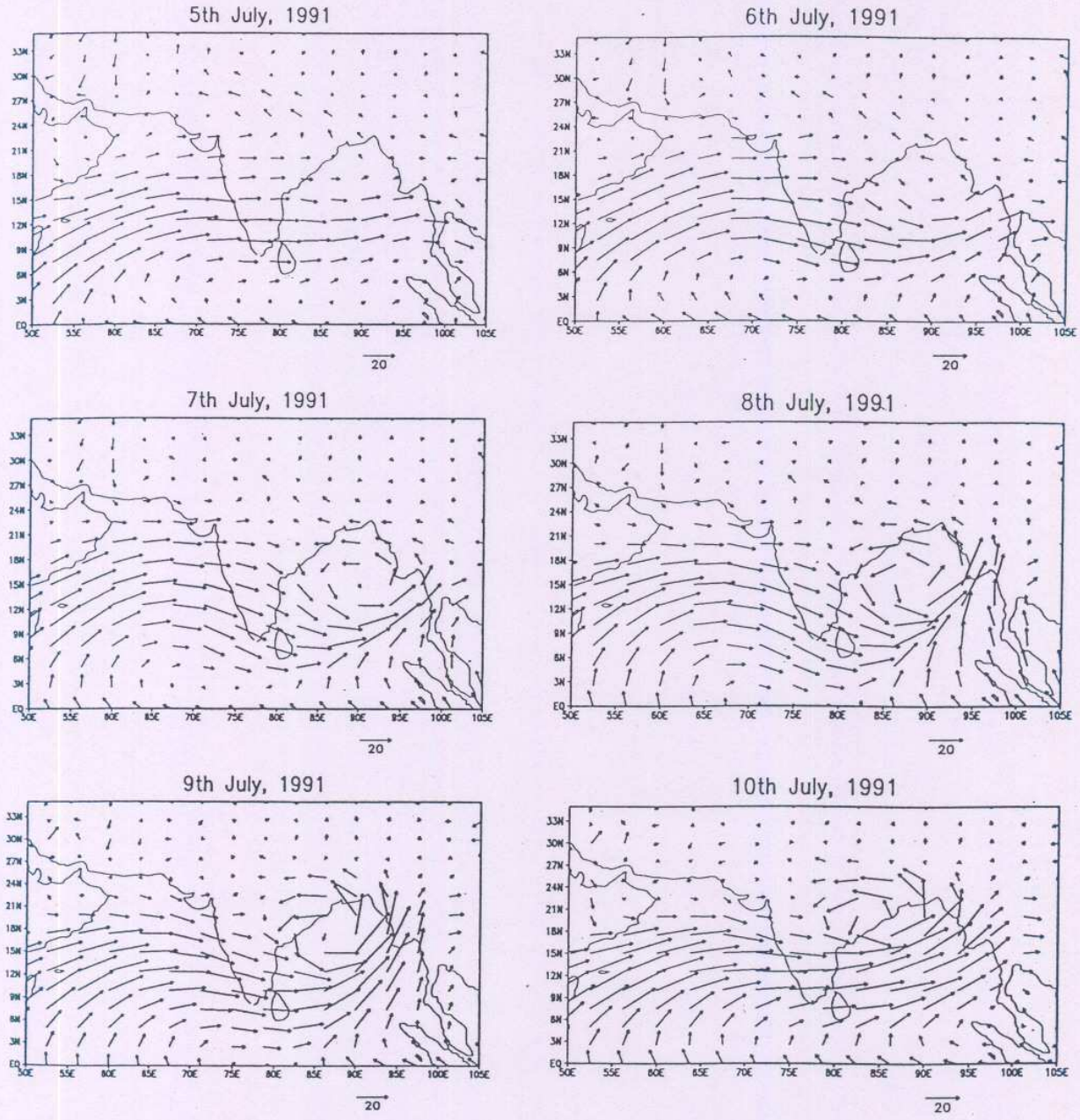

Fig. 3a Simulated Monsoon Depression by the Hadley Centre Climate Model.
Wind at 850 hPa (m/s)

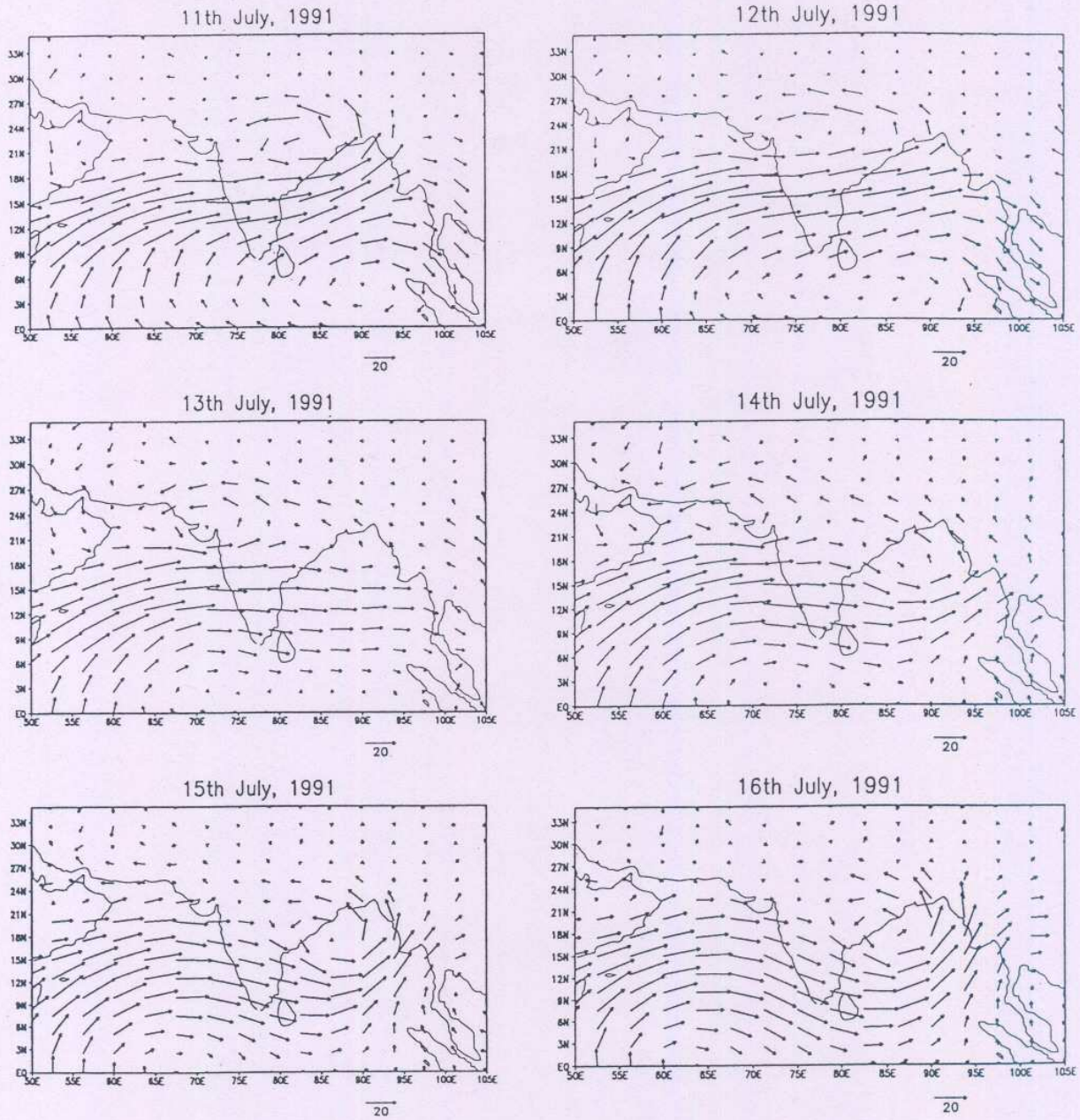

Fig. 3b :Simulated Monsoon Depression by the Hadley Centre Climate Model.
Wind at 850 hPa (m/s)

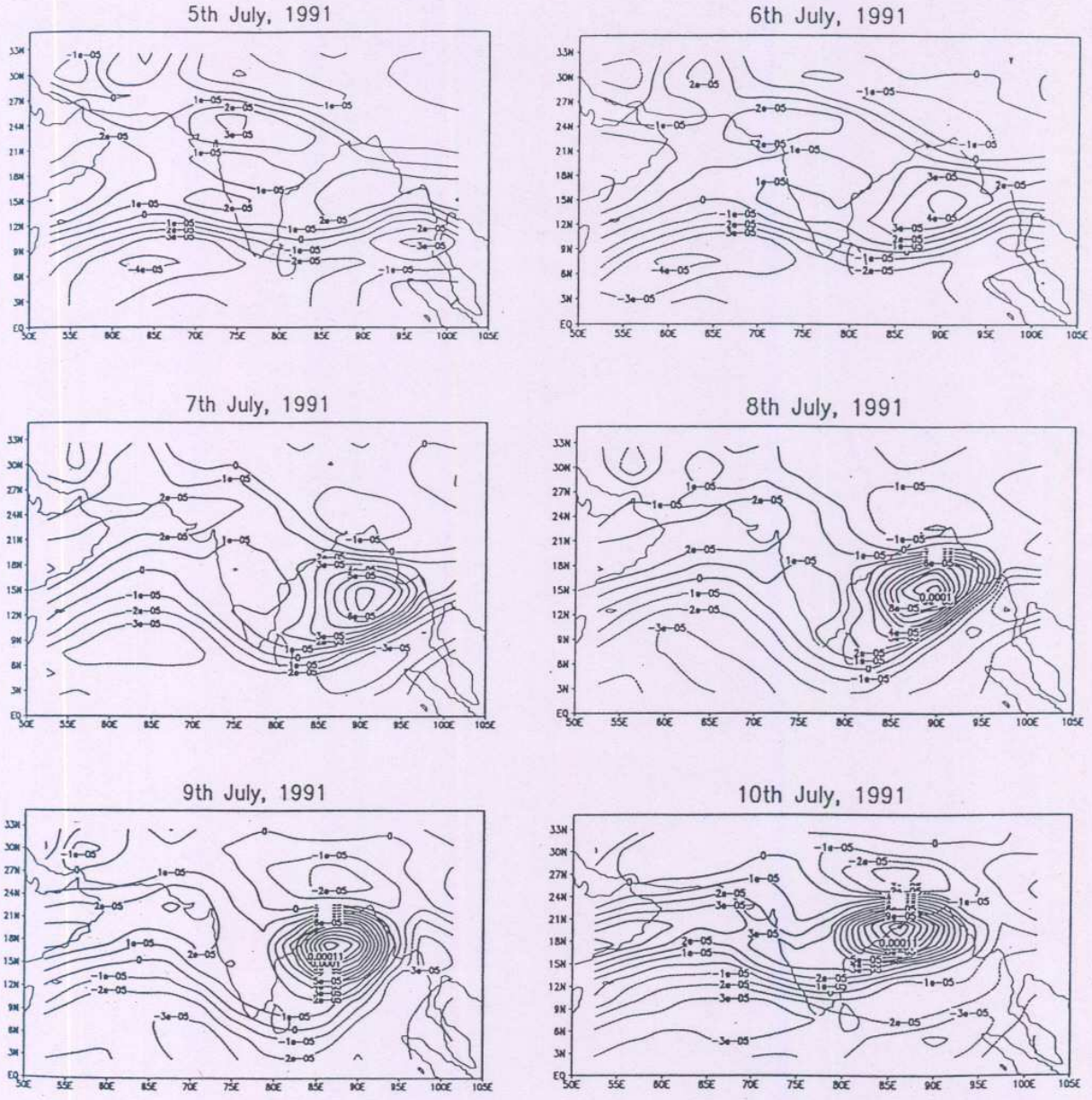

Fig. 4a Simulated Monsoon Depression by the Hadley Centre Climate Model. Relative Vorticity at 850 hPa. Contour intervals at .00001/s

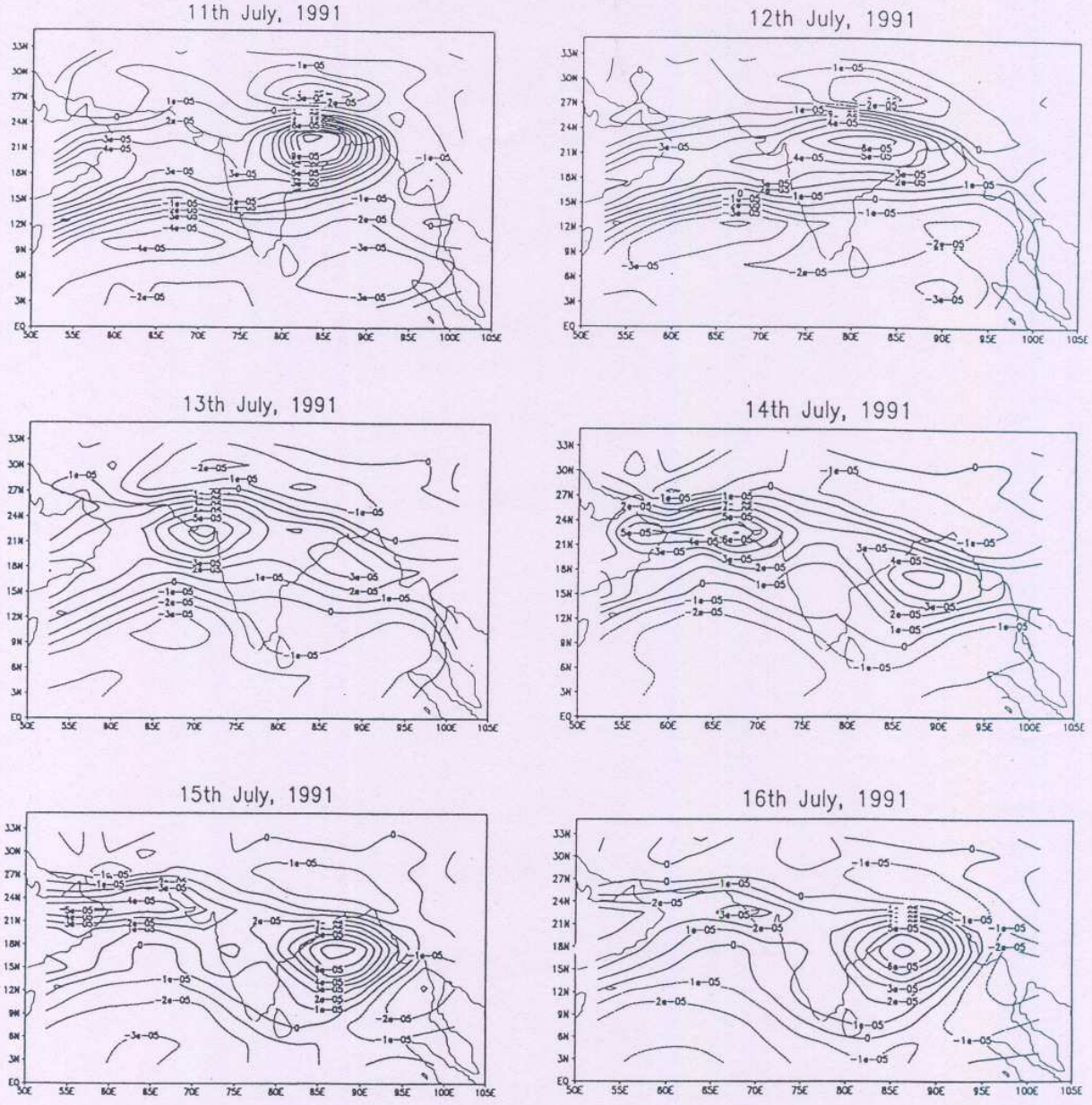

Fig. 4b Simulated Monsoon Depression by the Hadley Centre Climate Model.
Relative Vorticity at 850 hPa. Contour intervals at .00001/s

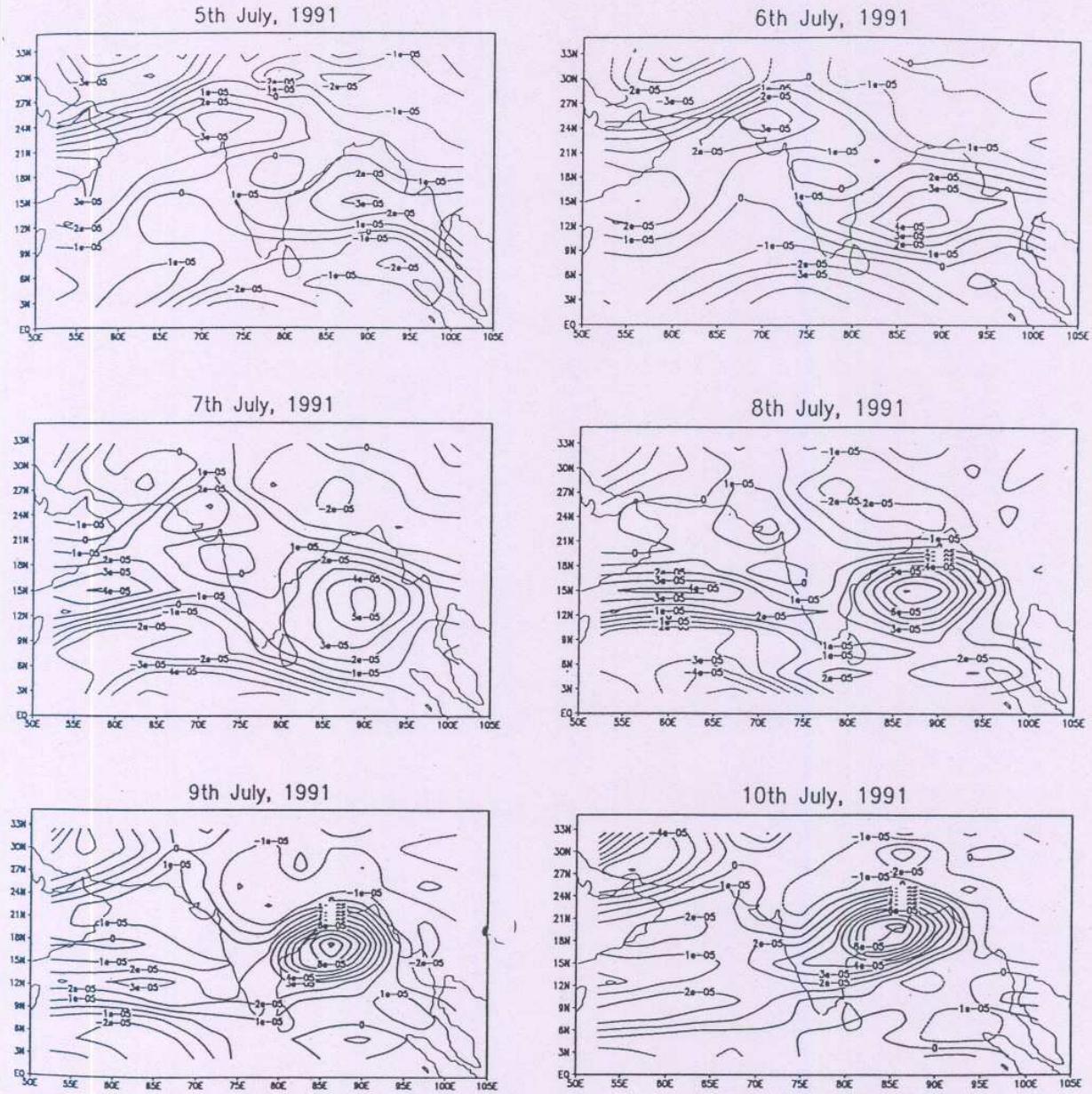

Fig. 5a :Simulated Monsoon Depression by the Hadley Centre Climate Model.
Relative Vorticity at 500 hPa. Contour intervals at .00001/s

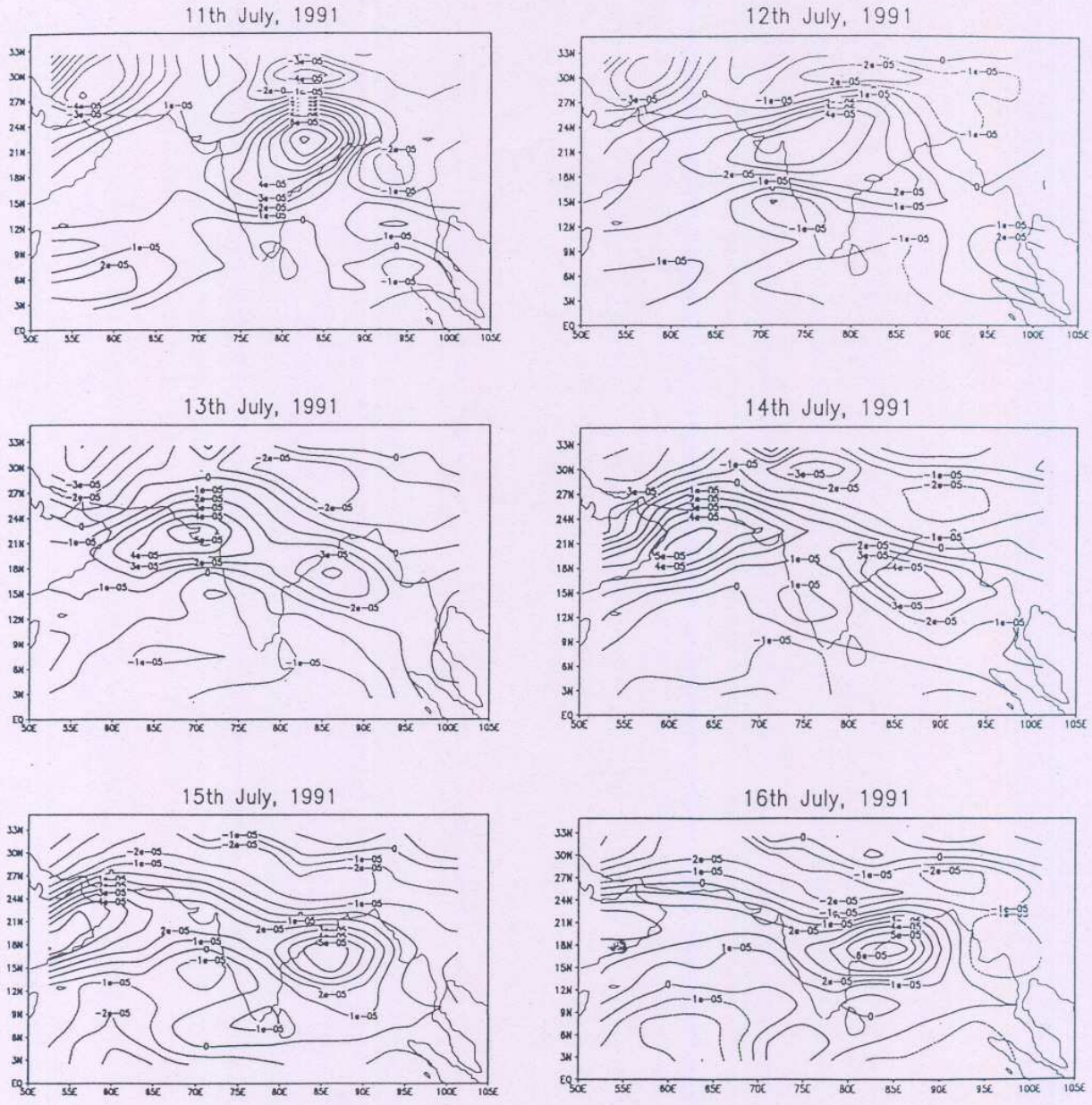

Fig. 5b :Simulated Monsoon Depression by the Hadley Centre Climate Model.
Relative Vorticity at 500 hPa. Contour intervals at .00001/s

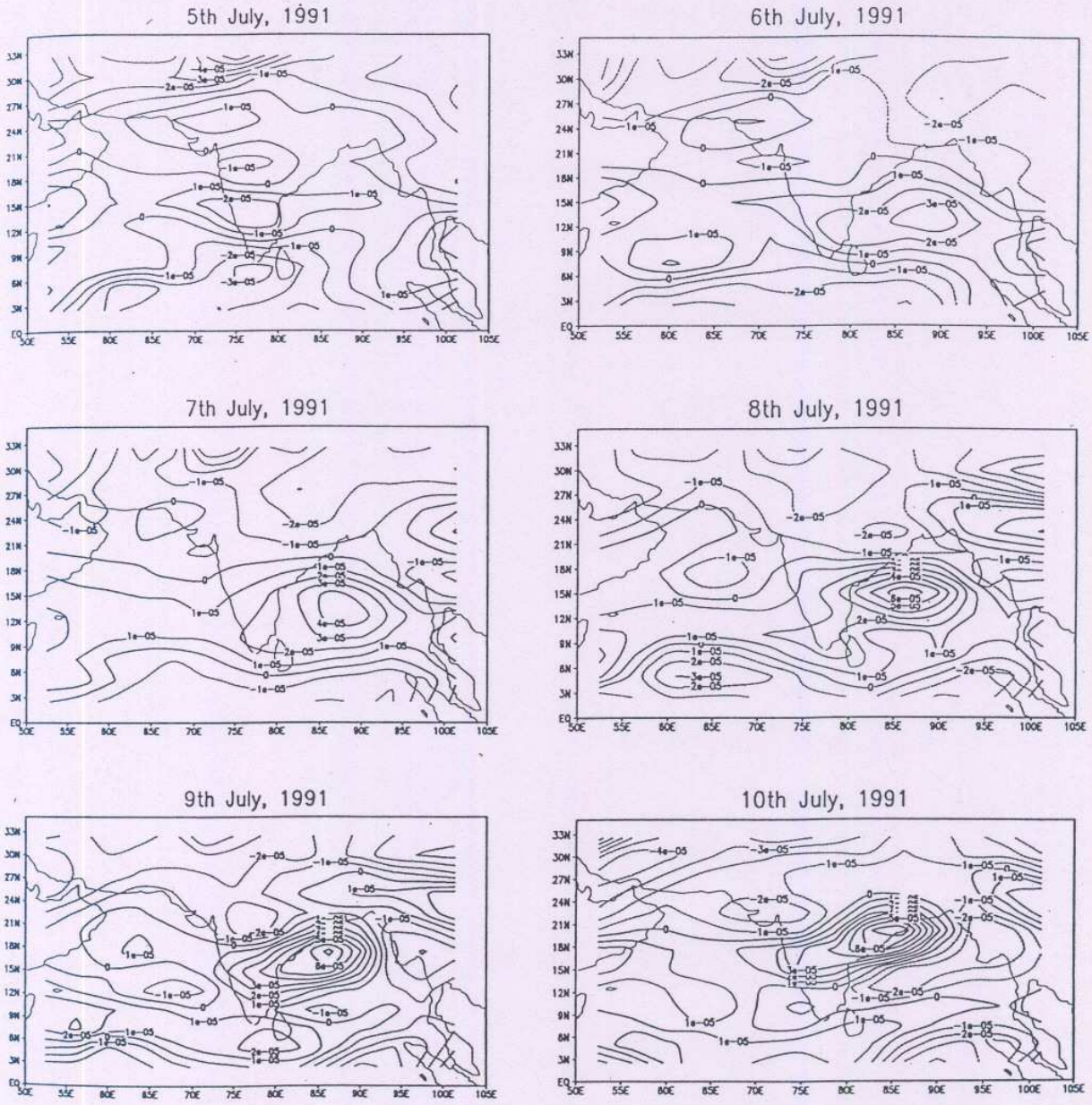

Fig. 6a: Simulated Monsoon Depression by the Hadley Centre Climate Model.
Relative Vorticity at 300 hPa. Contour intervals at .00001/s

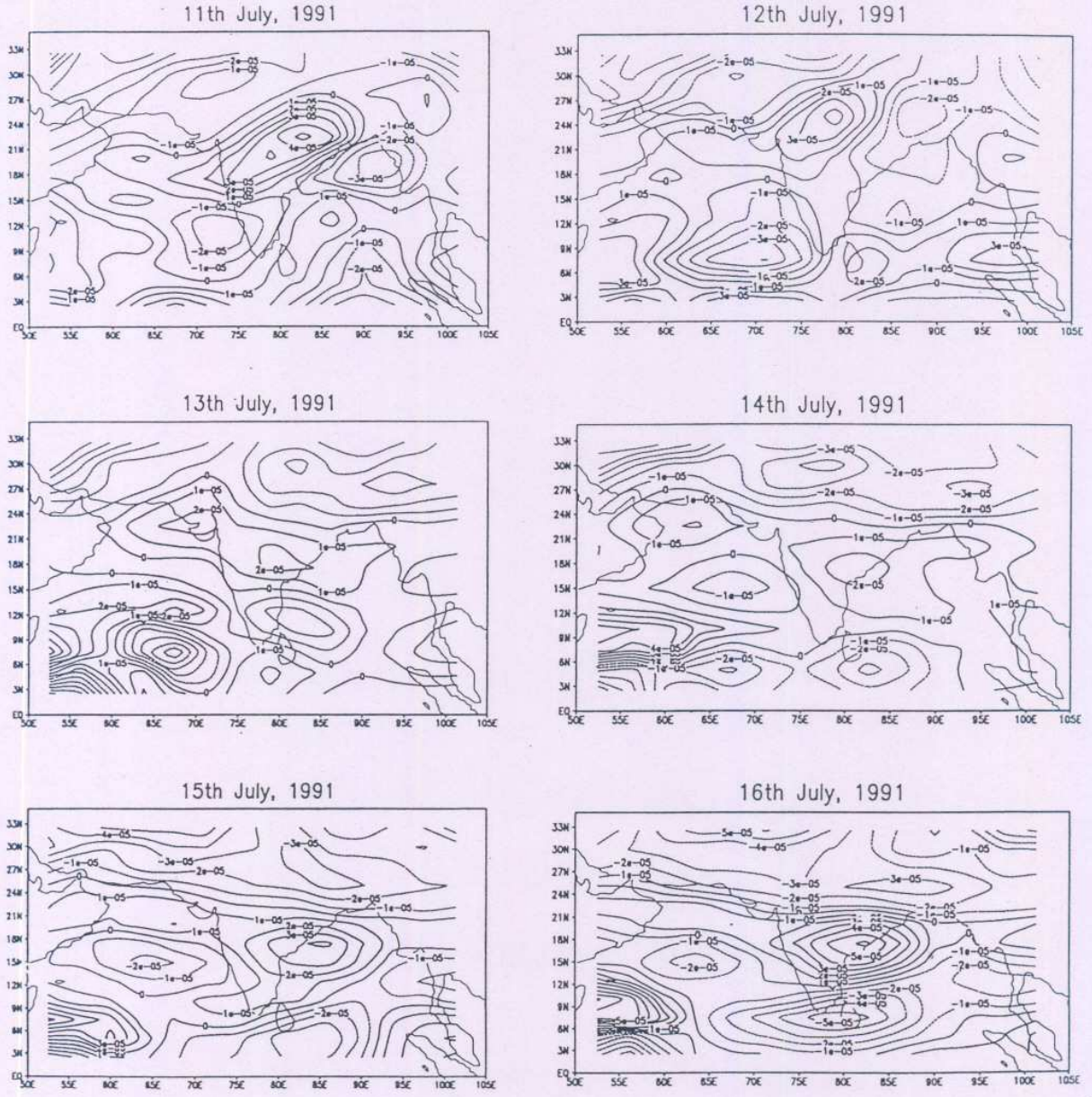

Fig. 6b :Simulated Monsoon Depression by the Hadley Centre Climate Model.
Relative Vorticity at 300 hPa. Contour intervals at .00001/s

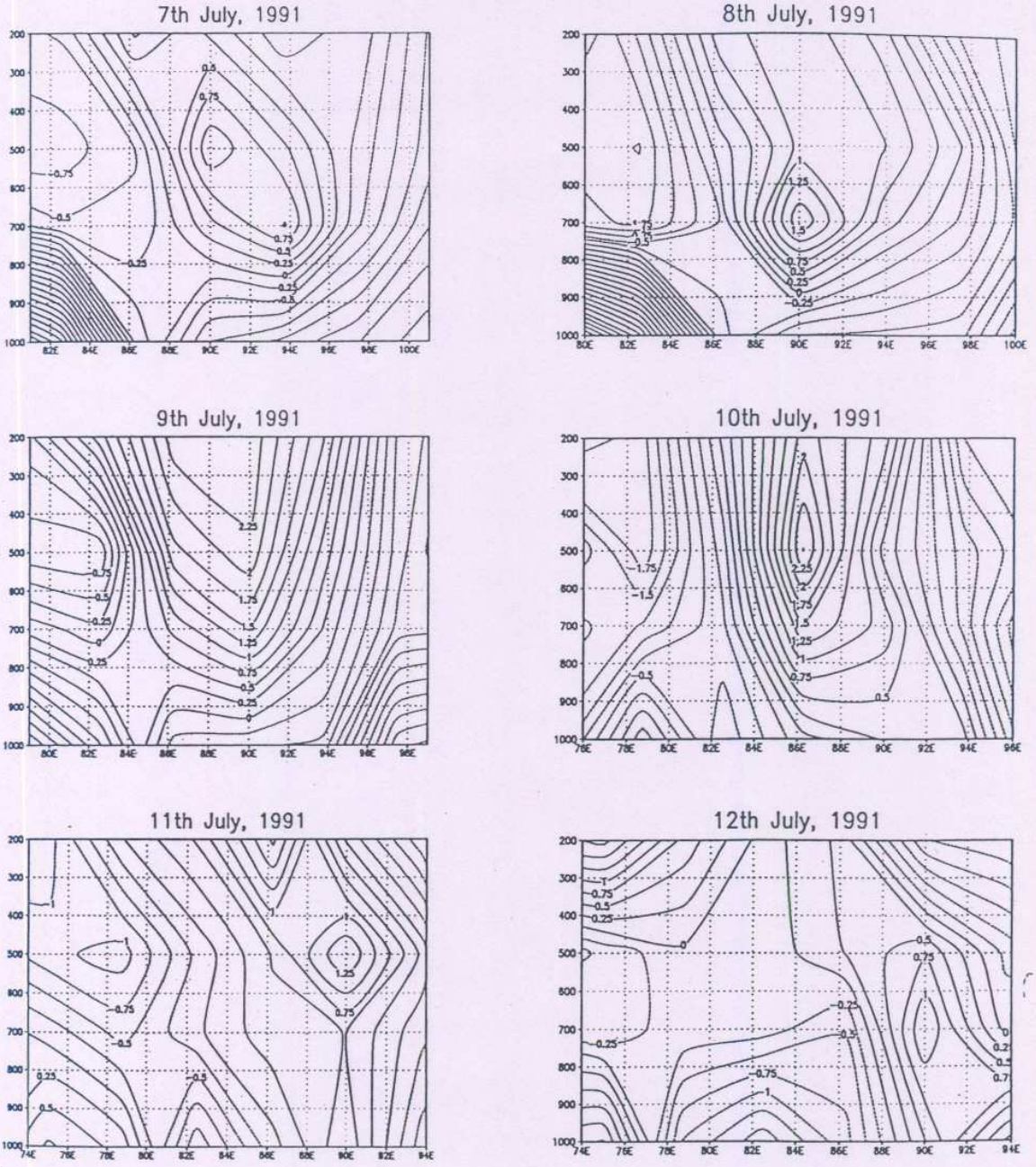

Fig. 7 : Simulated Monsoon Depression by the Hadley Centre Climate Model.

Distribution of Temperature Anamoly (C) in vertical

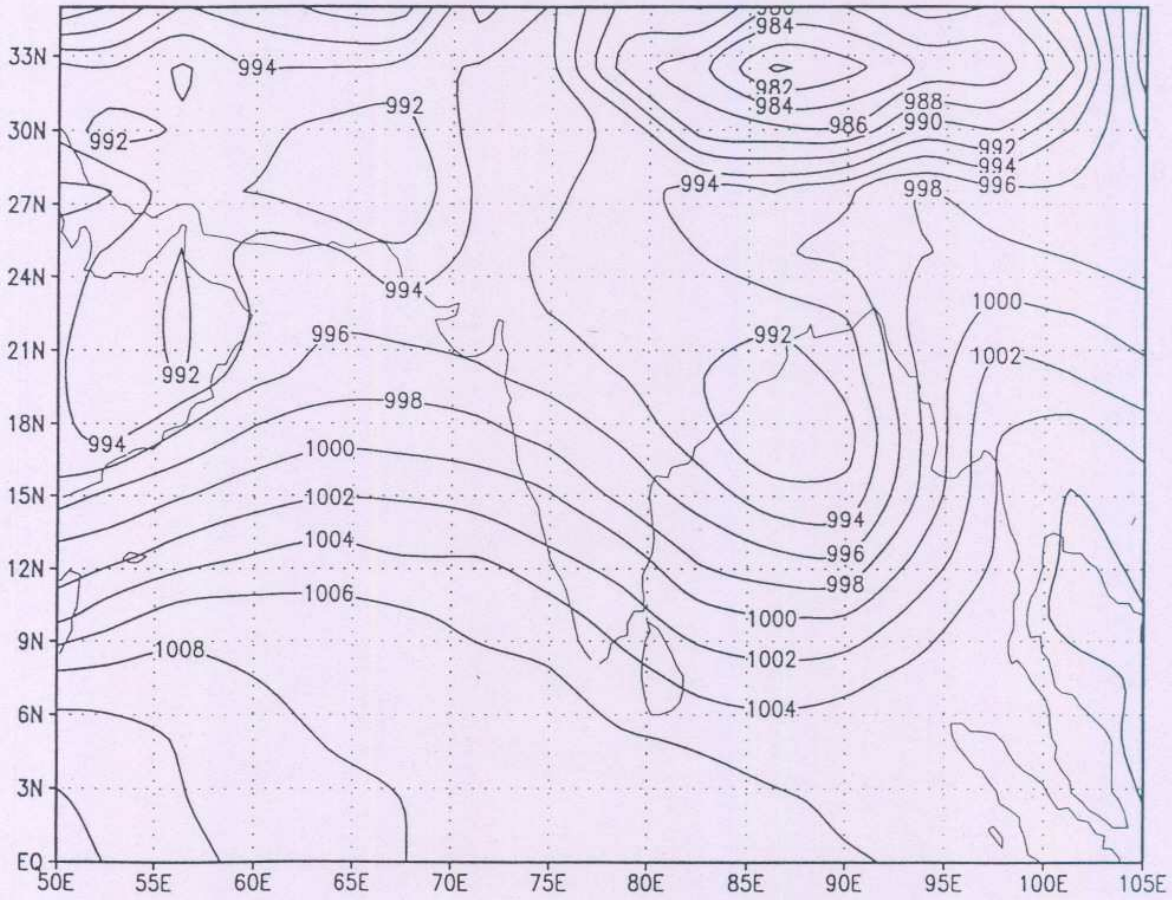

Fig. 8 Simulated Monsoon Depression by the Hadley Centre Climate Model. Composite PMSL from 8–11 July, 1991. Contour intervals at 2 hPa.

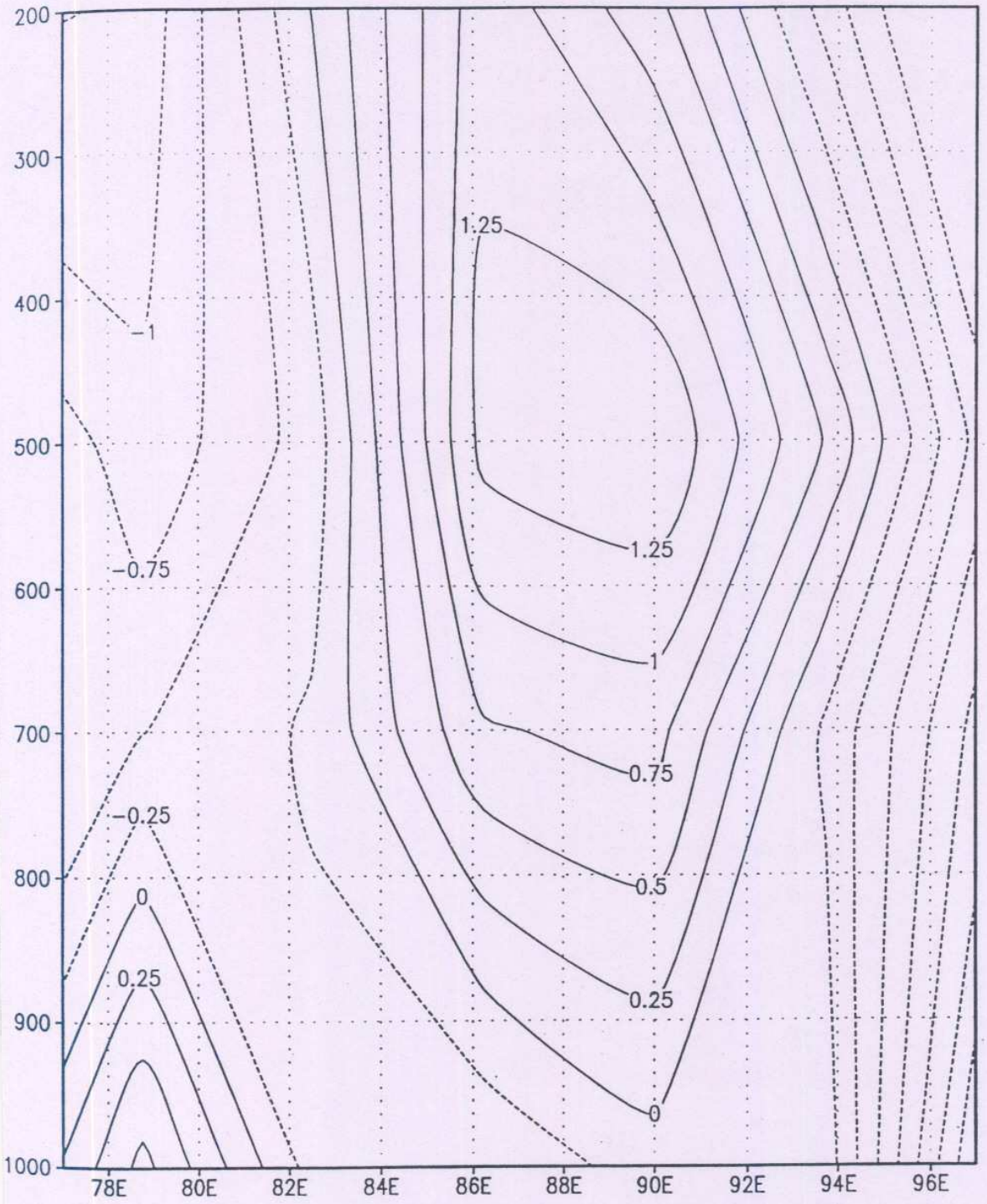

Fig. 9 : Simulated Monsoon Depression by the Hadley Centre Climate Model. Distribution of average (8–11th July, 1991) Temperature Anamoly in C

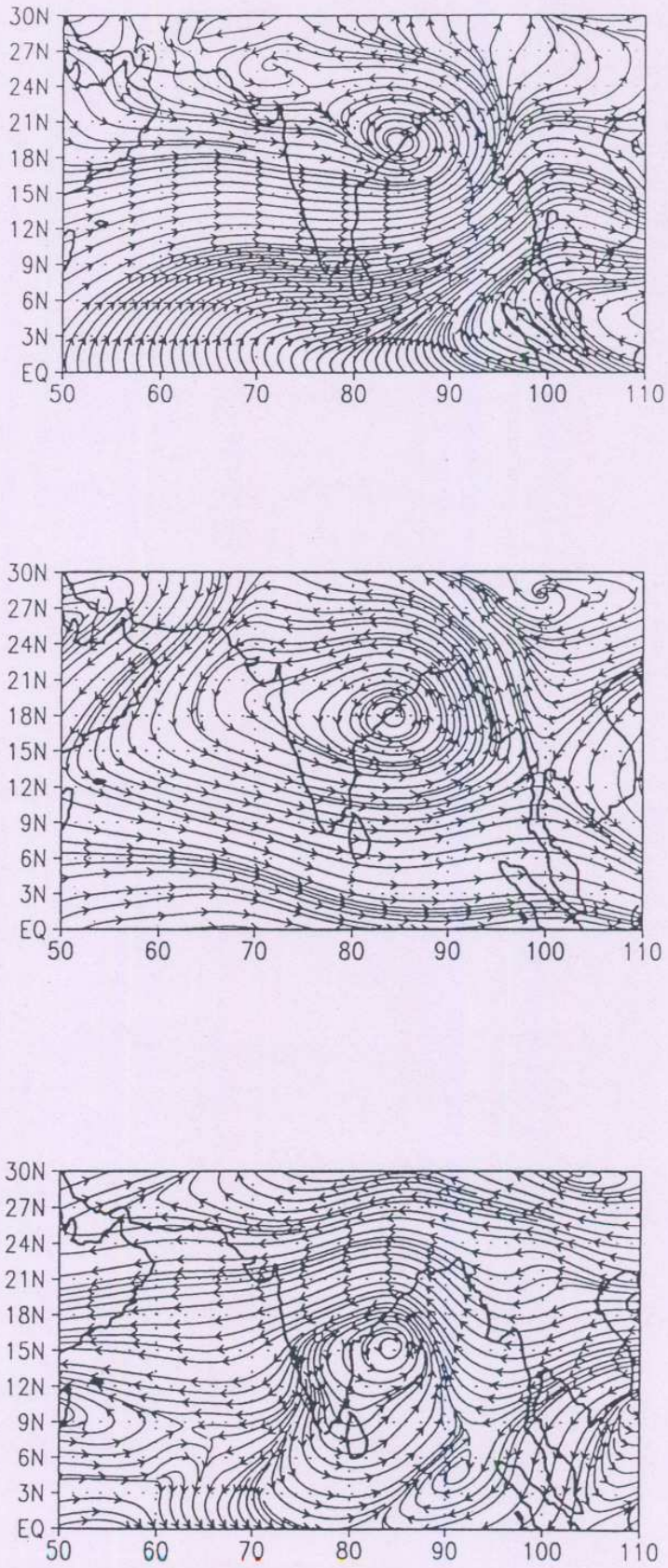

Fig. 10 :Simulated Monsoon Depression by the Hadley Centre Climate Model. Time averaged Streamlines (8th–11th July, 1991) at 850,500 &300 hPa (top to bott

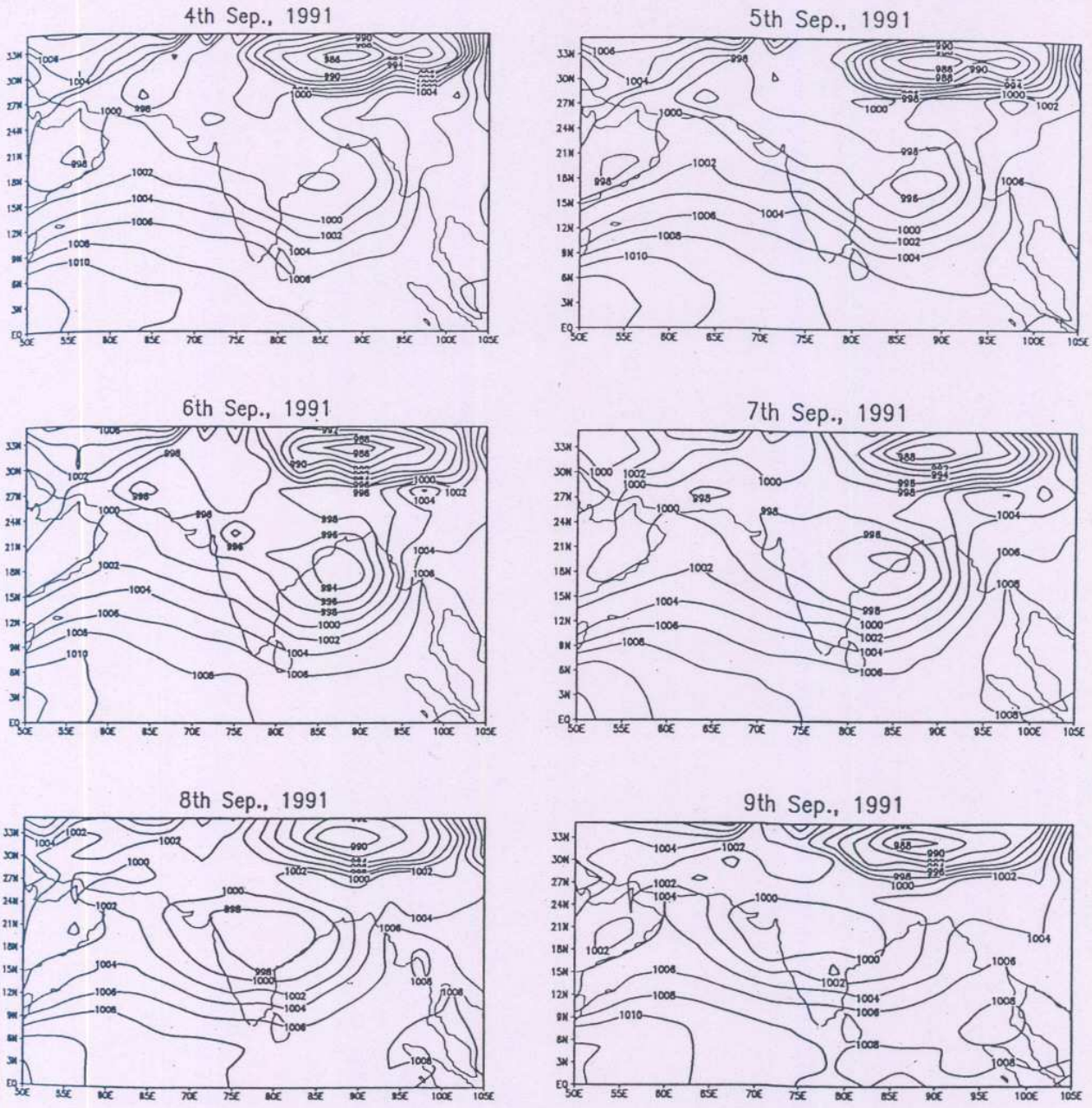

Fig. 11 :Simulated Monsoon Depression by the Hadley Centre Climate Model. Sea Level Pressure (hPa). Contour intervals at 2 hPa

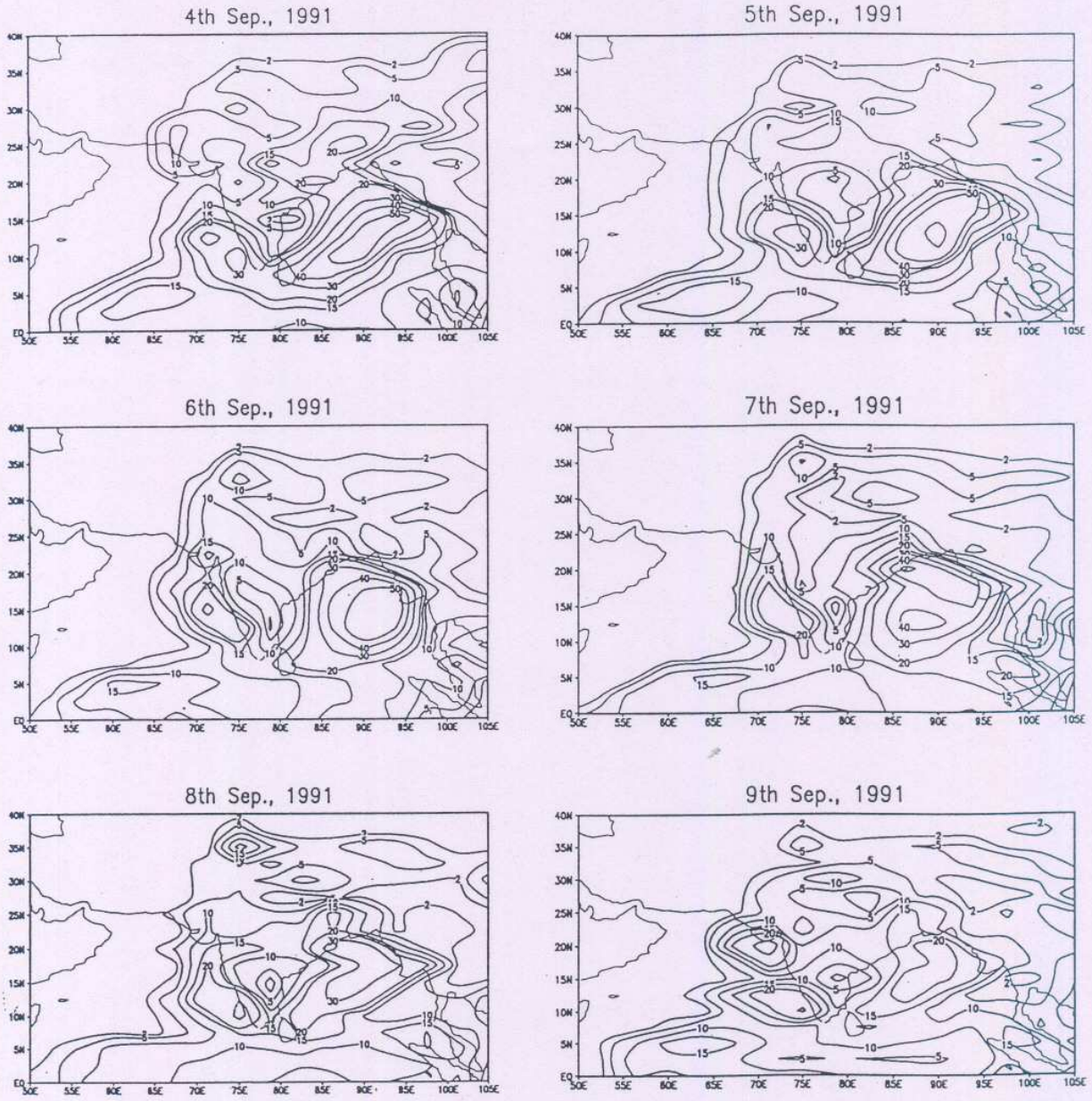

Fig. 12 Simulated Monsoon Depression by the Hadley Centre Climate Model.
Daily Rainfall (mm/day)

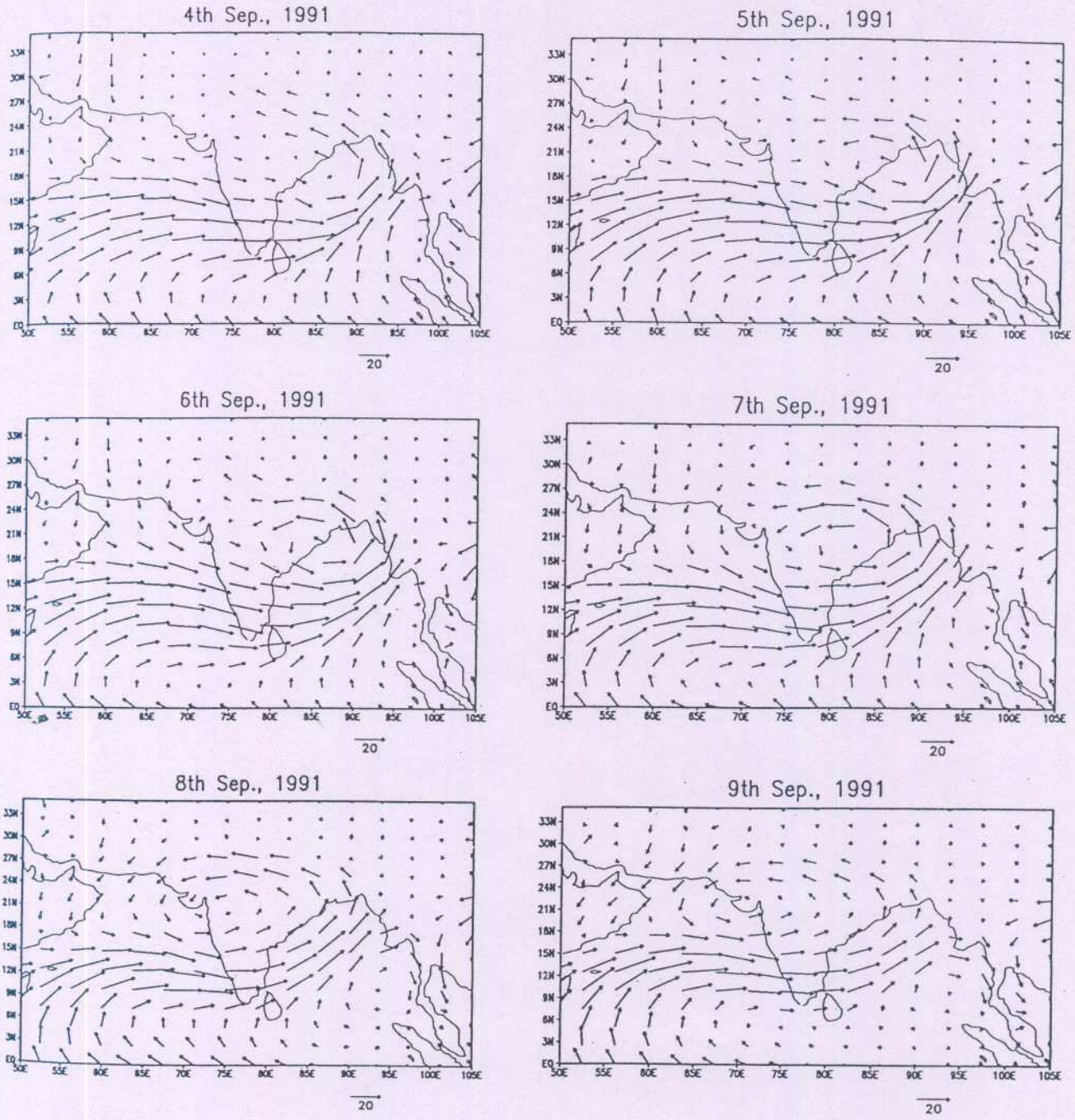

Fig.13 :Simulated Monsoon Depression by the Hadley Centre Climate Model.
Wind at 850 hPa (m/s)

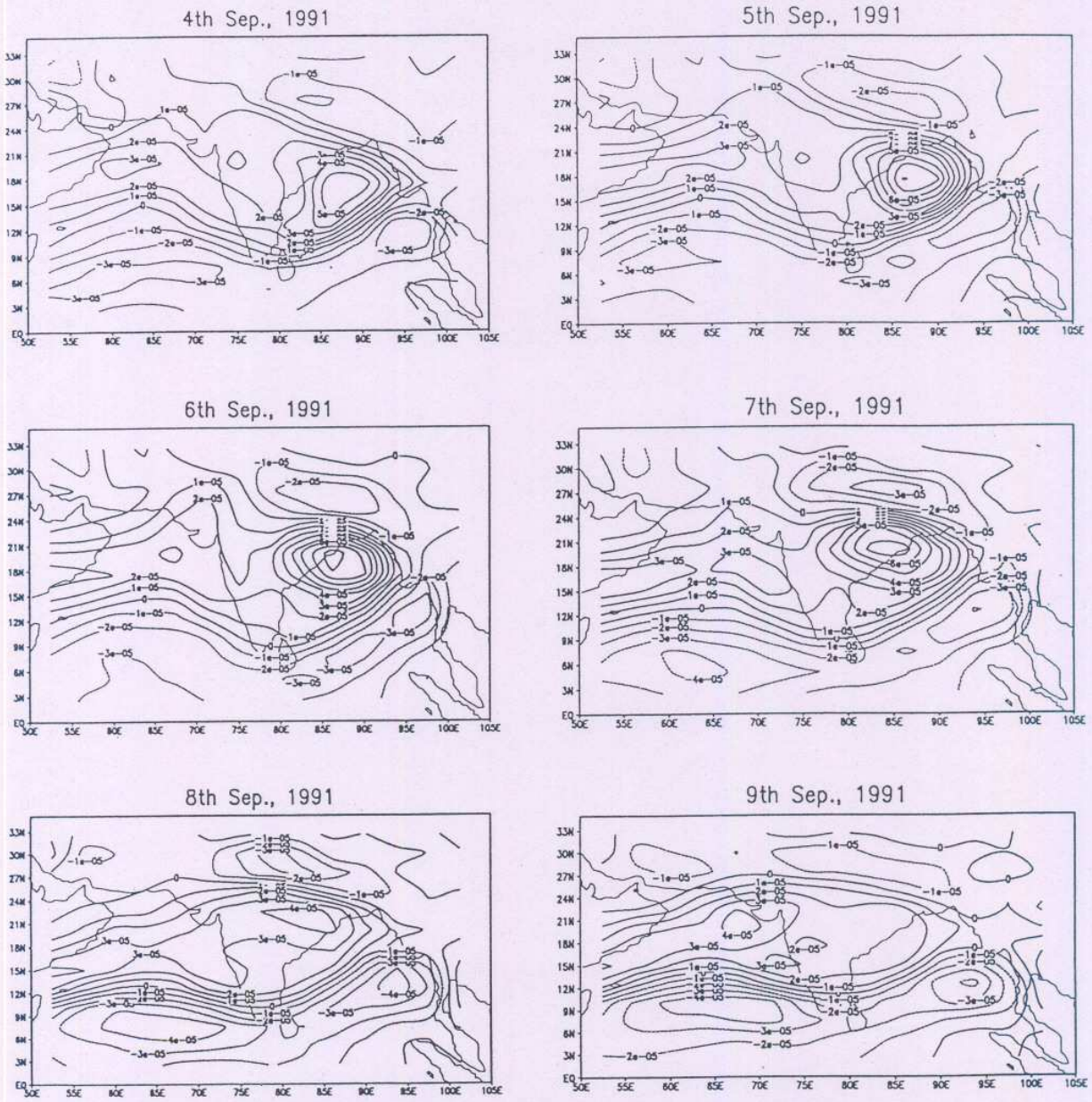

Fig. 14 :Simulated Monsoon Depression by the Hadley Centre Climate Model. Relative Vorticity at 850 hPa. Contour intervals at .00001/s

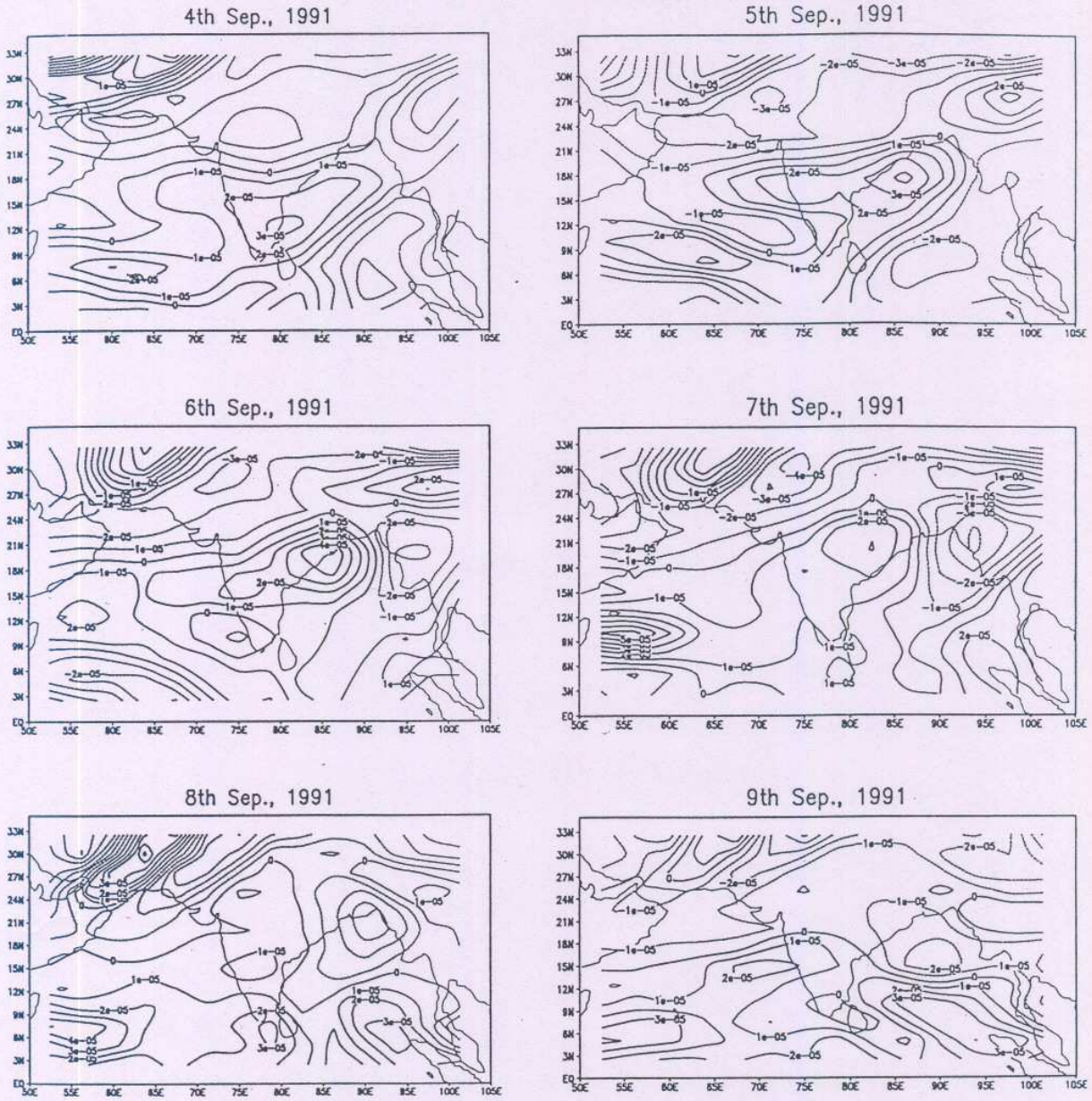

Fig. 15 :Simulated Monsoon Depression by the Hadley Centre Climate Model. Relative Vorticity at 300 hPa. Contour intervals at .00001/s